27 May 2010, 4:30 pm - 6:20 pm

Cyclic Torsional Shear Tests to Obtain Dynamic Soil Properties for Seismic Design of Road Embankments

Susumu Yasuda
Tokyo Denki University, Japan

Takafumi Tsuruda
Tokyo Denki University, Japan

CYCLIC TORSIONAL SHEAR TESTS TO OBTAIN DYNAMIC SOIL PROPERTIES FOR SEISMIC DESIGN OF ROAD EMBANKMENTS

Susumu Yasuda
Tokyo Denki University
Hatoyama, Hiki-gun, Saitama JAPAN 3500394

Takafumi Tsuruda
Tokyo Denki University
Hatoyama, Hiki-gun, Saitama JAPAN 3500394

ABSTRACT

Many road embankments have suffered damage during past earthquakes. The authors took soil samples from several embankments and conducted laboratory tests to demonstrate the mechanism of the damages and study appropriate seismic design methods. In the laboratory tests, cyclic torsional shear tests were carried out to obtain undrained cyclic strength, excess pore water pressure and shear modulus after cyclic loading of embankment soils. Test results showed a unique relationship between Plasticity Index and undrained cyclic strength is existed. Relationship between excess pore water pressure ratio and safety factor against liquefaction is also influenced by Plasticity Index. Then appropriate seismic design methods by applying these test results are discussed.

INTRODUCTION

In Japan, many road embankments have suffered damage during past earthquakes. In the design of road embankments, inclination of slopes, height and density of embankments are decided by empirical methods or stability analyses. Seismic force is rare to be considered in the design because embankments are easy to restore if the embankments are settled or slid. However, it becomes necessary to consider the behaviour of embankments under very strong shaking motion such as Level 2 shaking motion. Deformation of embankment due to earthquake may be evaluated by several analytical methods such as “ALID” and “Nemark’s method”. Then the authors conducted special soil tests to obtain appropriate dynamic soil properties for the analyses. The samples for the tests were taken at several sites where damage to embankments occurred during the 2004 Niigataken-chuetu earthquake and the 2007 Notohanto earthquake. Moreover a sample was taken at an expressway embankment near Tokyo.

SOIL SAMPLES AT THE DAMAGED EMBANKMENTS DURING TWO EARTHQUAKES

The 2004 Niigataken-chuetsu earthquake

On October 23, 2004, the Niigataken-chuetsu earthquake, of M_j=6.8, occurred. The maximum surface acceleration recorded

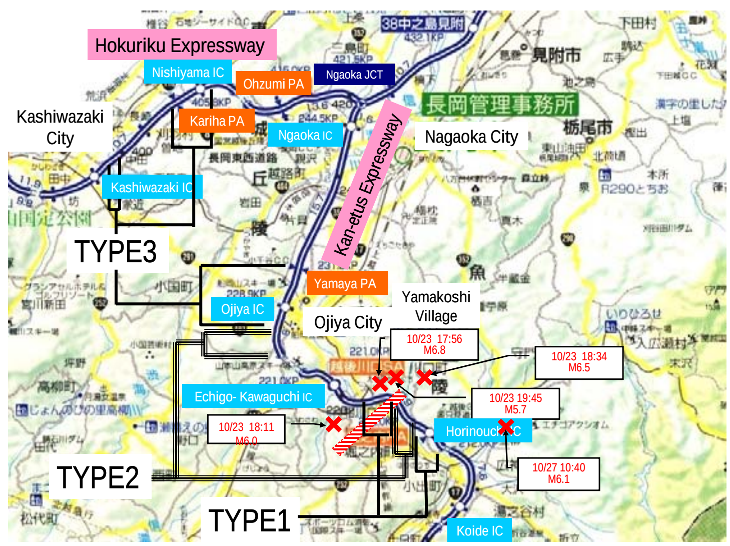

Fig. 1. Route map of Kan-etsu and Hokuriku Expressways and zones damaged during the Niigataken-chuestu and Niigataken-chuetsu-oki earthquakes (Yasuda and Fujioka,2009)

at Kawaguchi Town was 1,722 Gals. This earthquake caused serious damage to the embankments of Kan-etsu Expressway. This was the first time that an earthquake caused severe damage to the embankments of national expressways. In the seriously damaged area, damages to embankments are divided into three types as shown in Fig. 1 (Ohkubo, Fujioka and Yasuda, 2009):

(1) Type 1: Serious slide of the embankment on the sloping ground as shown in Fig. 2 (a) ;

(2) Type 2: Settlement of the embankment on the level ground without obvious deformation of the ground as schematically shown in Fig. 2 (b);

(3) Type 3: Settlement of the embankment and the culvert on level ground with deformation of the ground, as schematically shown in Fig. 2 (c) .

Then the authors took soil samples at Ojiya where Type 3 failure occurred, and conducted torsional shear tests

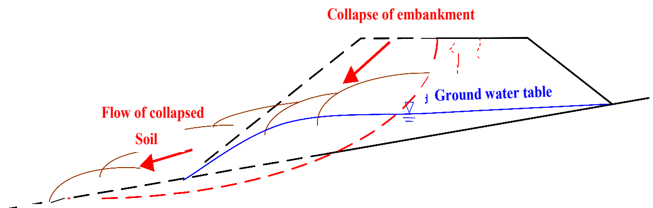

(a) Type 1: Serious slide of the embankment on the sloping ground

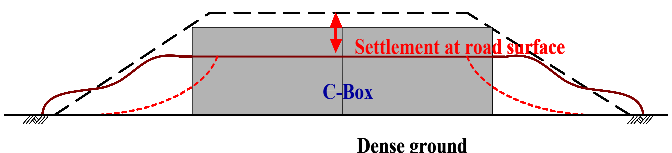

(b) Type 2: Settlement of the embankment on the level ground without the deformation of the ground

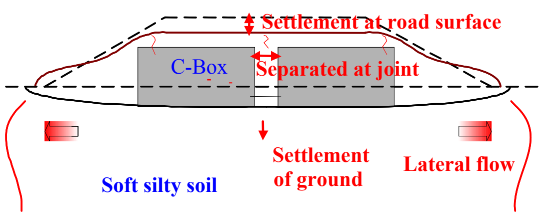

(c) Type 3: Settlement of the embankment and the culvert on the level ground with the deformation of the ground

Fig. 2. Classification of the damage to the embankment of Kan-etsu Expressway according to the mechanism of failure (Yasuda and Fujioka,2009)

<u>The 2007 Notohanto earthquake</u>

On March 25, 2007, the Noto-hanto earthquake, of M_j=6.9, occurred. The highway embankments of the Noto-yuryo road were very seriously damaged and huge slides occurred at 11 sites (Yasuda and Tanaka, 2010). Photos 1 and 2 show the slides at sites No. 9 and No. 32, respectively.

The authors took soil samples at the sites No. 9, No. 10 and No. 32, and conducted torisional shear tests. Moreover, as the similar slope failure occurred at an old-age institution near Noto-yuryo road in Anamizu Town, a soil sample was also taken at site.

Photo. 1. Slide of the embankment of Noto-yuryo road at site No. 9

Photo. 2. Slide of the embankment of Noto-yuryo road at site No. 32

TEST APPARATUS AND TEST PROCEDURE

Cyclic torsional shear test apparatus with cyclic and static loading devices, shown in Photo. 3, was used for the tests. Tested soils were the five samples taken at the damaged embankments mentioned above. In addition, the embankment soil at Atsugi of Tomei Expressway was tested also. These soils were compacted by tamping method in a mold to become hollow cylindrical specimens with 10 cm in outer diameter, 6 cm in inner diameter and 10 cm in height. Moisture content and degree of compaction of the soils were adjusted as optimum moisture content and 90 %, respectively.

Photo. 3. Hollow-cylindrical torsional test apparatus

Soil properties and grain size distribution curves of the soils are shown in Table. 1 and Fig. 3. Fines content of these soils are about 40 to 80 %. Plasticity index are about 10 to 30.

Table. 1. Soil properties of tested embankment soils

	Ojiya	Atsugi	Anamizu	No. 9	No. 10	No. 32
Maximum dry mass, ρ_{dmax} [g/cm^3]	1.530	1.116	1.317	1.703	1.395	1.316
Optimum moisture content, ω_{opt} [%]	24.5	43.0	32.8	17.9	32.8	34.6
Liquid limit, w_L [%]	35.5	58.8	64.7	53.0	70.5	49.2
Plastic limit, w_P [%]	28.4	38.8	40.1	32.2	42.7	35.4
Plasticity index, I_P	7.1	20.0	24.60	20.76	27.80	13.76
Fines content, F_C [%]	42.0	49.7	42.0	40.7	82.4	85.5
Natural water content, ω_n [%]	66.1	31.70				29.30

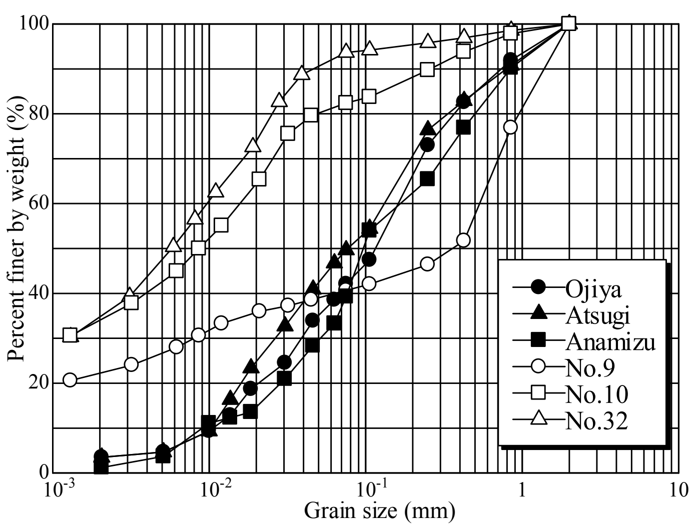

Fig. 3. Grain size distribution curves of tested soils

According to the previous damaged embankments, ground water levels were found inside the embankment as shown in Fig. 2 (a). It is estimated the soils upper and lower than the water level are partially saturated and fully saturated, respectively. Then the tests were carried out under two saturated conditions: i) partially saturated condition with the optimum moisture content, and ii) fully saturated condition. In the latter case, specimens were saturated by pouring water into the specimen. Then confining pressure was applied with back pressure. In the former case confining pressure was applied without pour water. Effective confining pressure, σ'_c was adjusted as 50 kPa.

20 cycles of cyclic loading with 0.1 cycle/sec was applied to the specimens as shown in Fig. 4 under undrained condition. After the cyclic loading, a monotonic loading was applied under undrained condition with a speed of 10 % of shear strain/minute. Time histories of shear stress, shear strain and pore water pressure during the monotonic loading were measured. About 4 to 8 specimens were used in one sample. And, different amplitude of cyclic loading was applied to each specimen to control safety factor against liquefaction (failure), F_L, which implies severity of liquefaction or failure, mentioned later. In addition, static tests to apply monotonic loading only were carried out. Hereafter, these tests were called as "static".

As mentioned above, different amplitude of cyclic loading was applied to each specimen. Then, relationships between cyclic stress ratio, τ_d / σ'_c and double amplitude of shear strain at 20 cycles, γ_{DA} (N_c=20) were plotted. And, the stress ratio to cause 7.5 % of shear strain by 20 cycles, R_L (γ_{DA}=7.5 %, N_L=20) was estimated. This stress ratio is same as the stress ratio to cause liquefaction, R_L (ε_{DA}=5 %, N_L=20) in cyclic triaxial tests for soils. Therefore, this stress ratio means liquefaction strength in soils.

In the liquefied specimen, shear strain increased with very low shear stress up to very large strain as schematically shown in Fig. 5 (a). Then, after a resistance transformation point (turning point), the shear stress increased comparatively rapidly with shear strain, following the decrease of pore water pressure. Stress-strain curves before and after the reference transformation point, γ_L can be presented approximately by a bilinear model with G_1, G_2 and γ_L :

$$\tau = G_1 \gamma \quad \text{for } \gamma < \gamma_L \tag{1}$$

$$\tau = G_1 \gamma_L + G_2 (\gamma - \gamma_L) \quad \text{for } \gamma > \gamma_L \tag{2}$$

where G_1 and G_2 are the shear module before and after the reference transformation point, respectively.

On the contrary, stress-strain curves of the clayey soils are different from those of liquefied sandy soils, as shown in Fig. 5 (b). Then the authors classified the shape of the stress-strain curves into two types as shown in Fig. 5 (a) and (b) (Yasuda et al., 2006). In clayey soils, it seems that large shear strain does not induce due to earthquake because some amount of resistance remains after cyclic loading. Therefore the authors defined shear modulus of softened soil, G_1 as the secant modulus at 1 % of shear strain as shown in Fig. 5 (b).

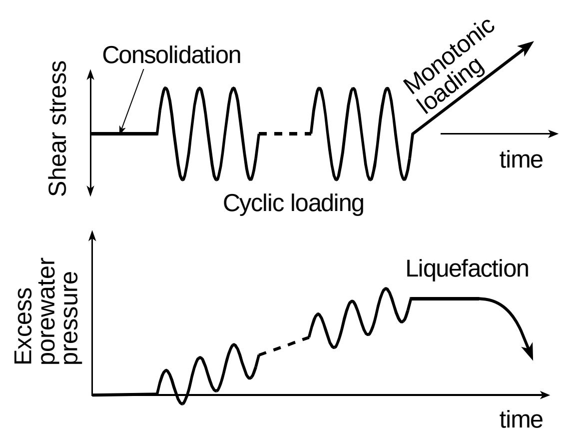

Fig. 4. Procedure of cyclic and monotonic loadings

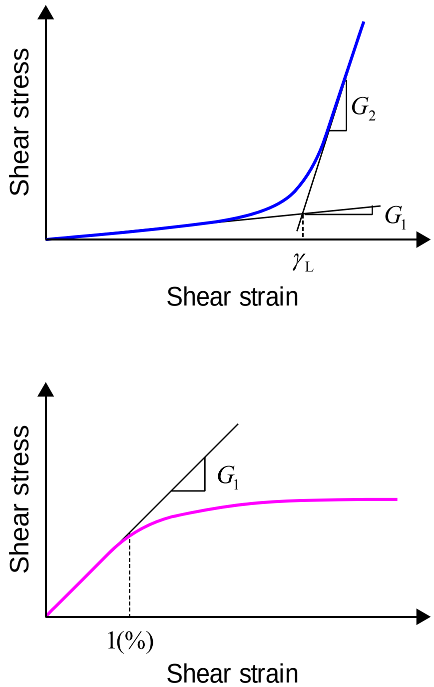

Fig. 5. Definition of G_{0i}, G_1 and γ_L

TEST RESULTS

Typical time histories of shear stress, shear strain, and excess pore water pressure during cyclic loading and monotonic loading for the Ojiya soil are shown in Figs. 6 to 9. In the fully saturated specimen express pore water pressure ratio increased up to 1.0 due cyclic loading. On the contrary, express pore water pressure ratio did not increase up to 1.0 in the partially saturated specimen. In the fully saturated specimen shear strain increased with low shear stress due to monotonic loading.

Fig. 10 shows relationships between double amplitude of shear strain and stress ratio for saturated and partially saturated specimens of Ojiya soil. The stress ratio to cause 7.5% of shear strain by 20 cycles, R_L (γ_{DA}=7.5 %, N_L=20) was estimated based on these relationships. Fig. 11 shows relationships between R_L (γ_{DA}=7.5 %, N_L=20) thus determined and Plasticity Index I_P. As shown in the figure, R_L (γ_{DA}=7.5 %, N_L=20) increased with I_P. And, the R_L for partially saturated specimens are larger than the R_L for fully saturated specimens. Fig. 12 shows relationships between excess pore water pressure ratio, $\Delta u/\sigma'_c$ at 20 cycles and safety factor against liquefaction, F_L. Excess pore pressure ratio deceased with F_L. Then the excess pore water pressure ratio at F_L=1, $\Delta u/\sigma'_c$ (F_L=1) were plotted on Fig. 13 with I_P. $\Delta u/\sigma'_c$ decreased with the increase of I_P for fully saturated specimens. This means that some resistance remains if I_P is large even though large shear strain induces. For partially saturated specimens, $\Delta u/\sigma'_c$ was less than 1 and decreased with I_P.

Fig. 14 shows relationships between shear modulus, G_1 and safety factor against liquefaction, F_L. Yasuda et al. (2006) conducted many torsional shear tests and proposed the relationship between F_L, R_L and G_1/σ'_c as shown as the curve in Fig. 15. Test data for F_L=1 in this study were plotted in the figure. Though the data are scattered, tested data for both fully saturated and partially saturated soils were plotted on near the proposed curve.

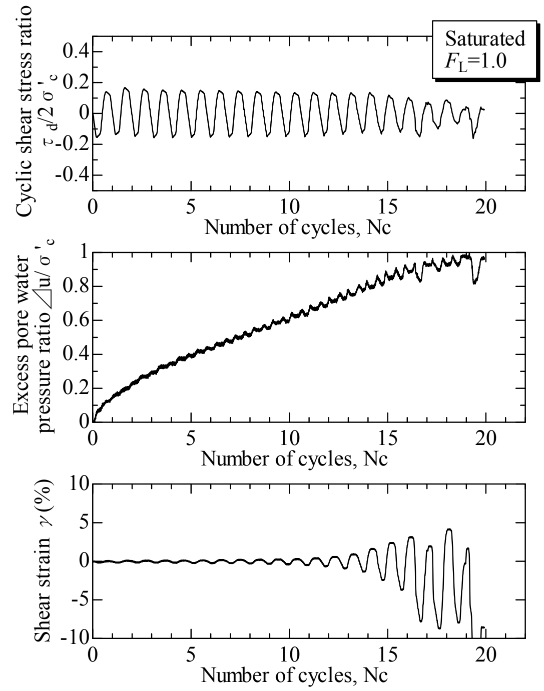

Fig. 6. Typical test results during cyclic loading of the fully saturated embankment soil at Ojiya

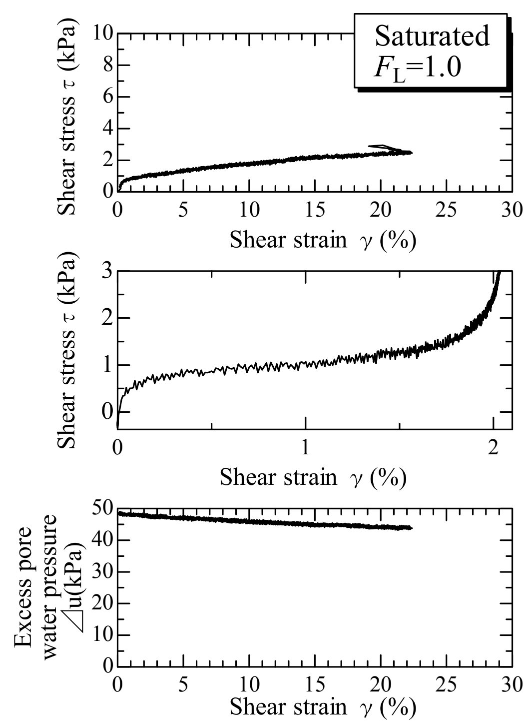

Fig. 7. Time histories of shear stress and excess pore water pressure during monotonic loading after cyclic loading for the embankment soil at Ojiya

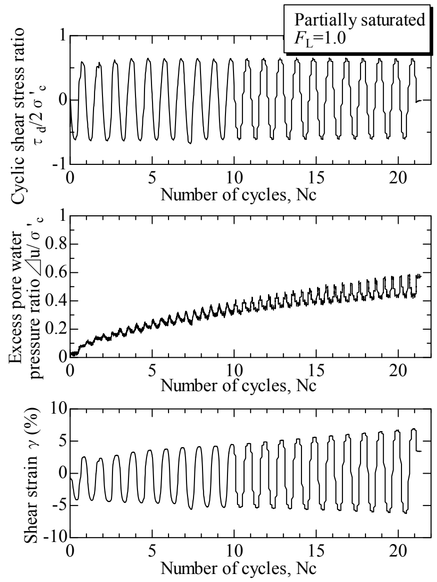

Fig. 8. Typical test results during cyclic loading of the partially saturated embankment soil at Ojiya

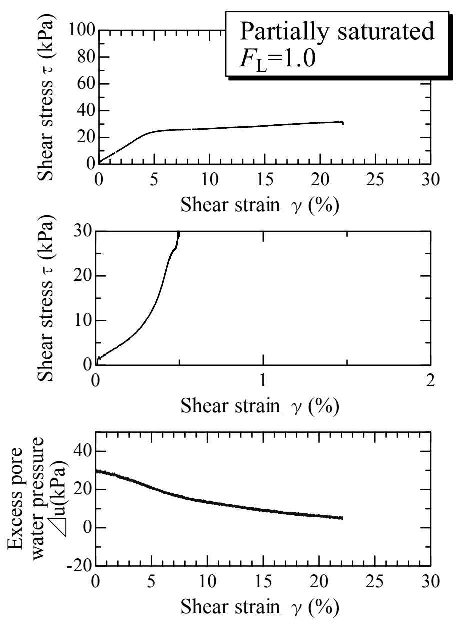

Fig. 9. Time histories of shear stress and excess pore water pressure during monotonic loading for the embankment soil at Ojiya

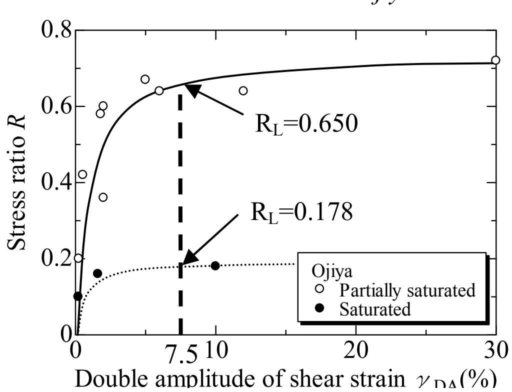

Fig. 10. Relationships between R and γ_{DA}

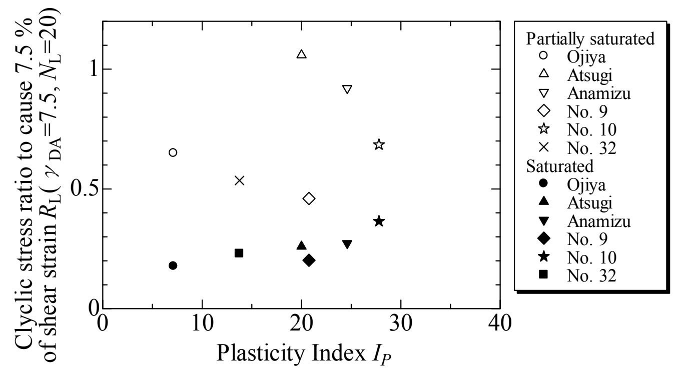

Fig. 11. Relationships between R_L (γ_{DA}=7.5 %, N_L=20) and I_P

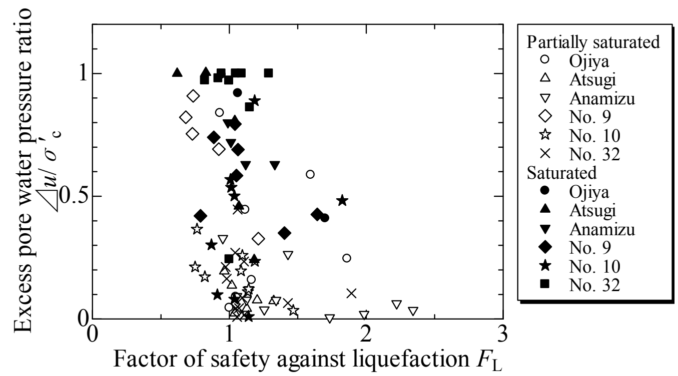

Fig. 12. Relationships between $\Delta u/\sigma'_c$ and F_L

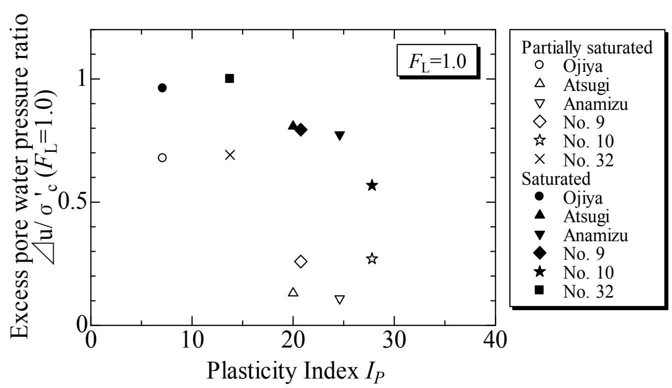

Fig. 13. Relationships between $\Delta u/\sigma'_c$ (F_L=1.0) and I_P

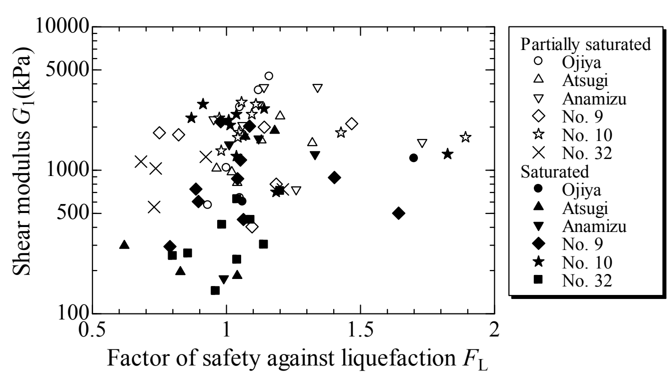

Fig. 14. Relationship between G_1 and F_L

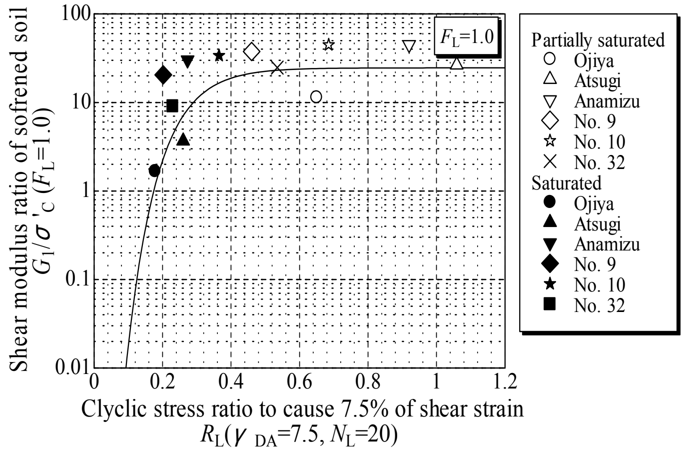

Fig. 15. Relationships between G_l/σ'_c and R_L (γ_{DA}=7.5 %, N_L=20)

DISCUSSION ON APPRPPRIATE SEISMIC DESIGN BY APPLYING TEST RESULTS

In the cuurent seismic design of embankments, stability analyses are conducted to deside the height and slope angle of the embankment. However, it becomes necessary to design not stability but deformation of the embankment in performance based design. As shown in the damage during the 2004 Niigataken-chuetu earthquake, mentioned before, there are mainly two deformation patterns; i) sliding failure, and ii) slump failure. In the sliding failure, sliding displacement can be evaluated by Newmark's method (Yasuda and Fujioka, 2009). On the contrary, slump dispacement can be evaluated by some deformation analyses such as ALID (Yasuda et al, 1999). Test results conduced here can be applied to the two methods as follows:

i) Newmark's method: relationships between F_L and $\Delta u/\sigma'_c$, and I_p and $\Delta u/\sigma_c'$.
ii)ALID: relationship between F_L, R_L and G_l/σ'_c

CONCLUSION

Cyclic torsional shear tests were carried out to examine cyclic shear strength and shear modulus after cyclic loading of saturated and partially saturated embankment soils of expressway embankments during previous earthquakes. Following are conclusions.

(1) Cyclic shear strength and shear modulus after cyclic loading of partially saturated soils are greater than those of saturated soils.
(2) Strength and shear modulus are affected by Plasticity Index I_P.
(3) Drainage of water from embankment is important not to saturate embankment soils.

REFERENCES

Ohkubo, K., Fujioka, K. and Yasuda, S . [2009] , "Slump failure of highway embankments during the 2004 Niigataken-chuetsu earthquake", *Earthquake Geotechnical Case Histories for Performance-Based Design: ISSMGE TC4 2005-2009 Term Volume*, CRC Press, pp. 71-82.

Yasuda, S., Yoshida, N., Adachi, K., Kiku, H., and Gose, S. [1999], "A simplified analysis of liquefaction induced residual deformation", *Proc. of the 2nd International Conference on Earthquale Geotechnical Enfineering*, pp. 555-560.

Yasuda, S., Inagaki, M., Nagao, K., Yamada, S. and Ishikawa, K.. [2006], "Analysis for the deformation of the damaged embankments during the 2004 Niigakaken-chuetsu earthquake by using stress-strain curves of liquefied sands or softened clays", *Soil Stress-Strain Behavior: Measurement, Modeling and Analysis, A Collection papers of Geotechnical Symposium in Roma*, Springer, pp. 663-672.

Yasuda, S. and Fujioka, K. [2009]. "A study on the method for the seismic design of expressway embankments", *Earthquake Geotechnical Engineering Satellite Conference, XVIIth International Conference on Soil Mechanics & Geotechnical Engineering*.

Yasuda, S, and Tomohiro, T [2009], "Geotechnical aspects of recent Japan earthquakes", *Fifth International Conference on Recent Advances in Geotechnical Earthquake Engineering and Soil Dynamics*. (in press)